Available online at www.sciencedirect.com

SCIENCE DIRECT

Genomics 87 (2006) 93 – 103

GENOMICS

www.elsevier.com/locate/ygeno

Hepatocyte iron loading capacity is associated with differentiation and repression of motility in the HepaRG cell line

Marie-Bérengère Troadec [a], Denise Glaise [a], Guillaume Lamirault [b], Martine Le Cunff [b], Emilie Guérin [a], Nolwenn Le Meur [b], Lénaïck Détivaud [a], Pierre Zindy [c], Patricia Leroyer [a], Isabelle Guisle [b], Hélène Duval [d], Philippe Gripon [a], Nathalie Théret [c], Karim Boudjema [a,e], Christiane Guguen-Guillouzo [a], Pierre Brissot [a,f], Jean J. Léger [b], Olivier Loréal [a,*]

[a] *INSERM U522, IFR 140, University of Rennes 1, CHRU Pontchaillou, 35033 Rennes Cedex, France*
[b] *INSERM U533, 44035 Nantes Cedex, France*
[c] *INSERM U620, 35043 Rennes Cedex, France*
[d] *Service d'Anatomo-Pathologie, Hôpital Universitaire Pontchaillou, 35033 Rennes Cedex, France*
[e] *Département de Chirurgie Viscérale, Hôpital Universitaire Pontchaillou, 35033 Rennes Cedex, France*
[f] *Service des Maladies du Foie, Hôpital Universitaire Pontchaillou, 35033 Rennes Cedex, France*

Received 15 February 2005; accepted 27 August 2005
Available online 1 December 2005

Abstract

High liver iron content is a risk factor for developing hepatocellular carcinoma (HCC). However, HCC cells are always iron-poor. Therefore, an association between hepatocyte iron storage capacity and differentiation is suggested. To characterize biological processes involved in iron loading capacity, we used a cDNA microarray to study the differentiation of the human HepaRG cell line, from undifferentiated proliferative cells to hepatocyte differentiated cells. We were able to identify genes modulated along HepaRG differentiation, leading us to propose new genes not previously associated with HCC. Moreover, using Gene Ontology annotations, we demonstrated that HepaRG hepatocyte iron loading capacity occurred both with the repression of genes involved in cell motility, signal transduction, and biosynthesis and with the appearance of genes linked to lipid metabolism and immune response. These results provide new insights in the understanding of the relationship between iron and hepatocyte differentiation during iron-related hepatic diseases.

Keywords: Hepatocyte; Iron metabolism disorders; Cell differentiation; Cell cycle; Cell motility; Gene expression; cDNA microarrays; Microarray analysis; Hepatocellular carcinoma

Introduction

Hepatocytes play a key role in iron metabolism through: (i) the production of serum proteins including transferrin [1], ceruloplasmin [1], haptoglobin [2], hemopexin [3], and hepcidin [4]; (ii) their capacity to take up iron present in excess in plasma, especially the non-transferrin-bound iron species [5,6]; and (iii) the ability of hepatic cells to store excessive iron inside ferritin molecules [7]. In humans, hepatic iron overload diseases may occur, especially during genetic hemochromatosis linked to the C282Y mutation of the *HFE* gene ([8], review in [9]), and then lead to the development of cirrhosis and hepatocellular carcinoma [10]. Moreover, during non-iron-related chronic liver diseases such as viral hepatitis or alcoholic diseases, patients developing hepatocellular carcinoma frequently exhibit an increase in hepatic iron concentration in the nontumoral area of the liver compared to patients without hepatocellular carcinoma, whereas hepatocellular carcinoma cells, which are proliferating and dedifferentiated, are free of iron deposits [11,12].

All these data suggest that iron may play a role in hepatic carcinogenesis and, reciprocally, that iron metabolism in hepatocytes is strongly modulated by the hepatocyte proliferation and/or differentiation status.

Adult hepatocytes are involved in many biological processes including the detoxification of xenobiotics, secretion of

* Corresponding author. Fax: +33 2 99 54 01 37.
E-mail address: olivier.loreal@rennes.inserm.fr (O. Loréal).

0888-7543/$ - see front matter © 2005 Elsevier Inc. All rights reserved.
doi:10.1016/j.ygeno.2005.08.016

plasmatic proteins, glycolysis, lipid metabolism, and bile secretion. In addition, they are also the main target for viruses having hepatic tropism. The HepaRG cell line, previously obtained from a hepatocellular carcinoma complicating chronic hepatitis C, revealed original biological characteristics. Indeed, this cell line evolves from bipotent progenitor cells toward both hepatocyte-like and primitive biliary epithelial cells [13,14]. In contrast with other hepatocyte-derived human cell lines, a feature of this cell line is its capacity to evolve from a proliferative undifferentiated stage to a very high level of hepatocyte differentiation reflected by the expression of xenobiotic detoxification pathways. This kinetics parallels liver development. Finally, HepaRG is thus far the only cell line able to support hepatitis B virus infection [13] similarly to primary human hepatocytes [15]. Taken together, these results suggest that the HepaRG cell line is a valuable model mimicking adult hepatocytes. Thus, the HepaRG cell line can be used to characterize the relationship between iron and hepatocytes.

Therefore, our aim was to analyze, using a transcriptomic approach through a liver-dedicated cDNA microarray, the relationship between iron storage capacity and hepatocyte differentiation status in the HepaRG cell line. Our data enabled us to identify the differentiation steps that are associated with iron storage capacity and to highlight biological processes modulated at these steps.

Results

Human liver microarray

The four cDNAs libraries obtained from human hepatocellular carcinoma and HepaRG cell line were used to build the human liver dedicated microarray. The median cDNA insert size of the 2436 selected clones was 489 bp. These clones, as well as a set of 36 PCR-amplified genes involved in iron metabolism, were representative of 584 distinct genes. Both human liver libraries and HepaRG libraries contributed 58 and 30%, respectively, of the genes, whereas 12% of the genes were found in both libraries. The involvement of these genes in different biological processes was evaluated at level 3 in Gene Ontology (GO) and the results are presented in Table 1. A total of 12 biological processes were represented by more than 8 genes. The most represented biological process was "metabolism" with cDNAs representing genes such as albumin (*ALB*) or the cytochrome p450 family. This cDNA microarray gave us the opportunity to analyze the relationship between iron storage capacity and hepatocyte differentiation process.

Table 1
Repertoire of the human liver dedicated microarray

Gene ontology terms: biological processes	% of annotated genes	Total array gene number
Metabolism	66.2	221
Cellular physiological process	35.6	119
Response to stimulus	23.4	78
Organismal physiological process	20.1	67
Cell communication	17.7	59
Regulation of physiological process	8.4	28
Regulation of cellular process	8.4	28
Death	6.6	22
Morphogenesis	6.3	21
Coagulation	3.0	10
Homeostasis	2.7	9
Regulation of enzyme activity	2.4	8
« Others »	7.2	24
Genes annotated at level 3		334
Unclassified		204
Total gene number		584

Level 3 Gene Ontology biological processes represented on the cDNA microarray. Some genes are annotated by several terms, and some others are not annotated. "Others" gathers biological processes representing each less than 2% of total array genes.

HepaRG differentiation kinetics

Based on both phenotype and morphologic criteria from phase-contrast microscopy observations [13,14] (Fig. 1A), we distinguished four distinct steps in the HepaRG differentiation process. At the first stage of differentiation, HepaRG cells presented a homogeneous epithelial phenotype [13] associated with intense cell proliferation. During the second stage, when reaching confluence, the cell proliferation rate decreased, despite the absence of any significant morphological changes. Morphologic and phenotypic changes appeared approximately 10 to 15 days postplating when cells were superconfluent, corresponding to the third stage of differentiation. Two cell populations appeared with polarized hepatocyte-like cell colonies with biliary canaliculi and biliary-like epithelial cells [14]. At the fourth stage, the addition of dimethylsulfoxide reinforced the hepatocyte morphology, including the presence of biliary canaliculi within hepatocyte-like cell colonies [13].

Identification of modulated genes

A lot of genes—from 140 to 221 genes depending on the considered step—were significantly modulated along the HepaRG differentiation process. The exhaustive list of significantly modulated genes is available at http://u522.rennes.inserm.fr/donnees/troadec.htm. We identified two clusters of co-regulated genes, those that were constantly significantly up-regulated and those that were down-regulated along HepaRG differentiation kinetics. These clusters are presented in Table 2. In the first group of down-regulated genes, we noted some genes implicated in cell growth, macromolecule metabolism, and biosynthesis, including elongation factors (e.g., *EEF1A1*) and ribosomal proteins (e.g., *RPL10* and *RPL2*). These genes, including three that were not annotated in GO regarding a biological process, had a similar expression profile. They are potentially involved in a common functional network.

In order to validate the results of our hybridizations, we tested 12 gene expression profiles at each differentiation stage by quantitative RT-PCR (Fig. 2). All of the up-regulated genes (*ADH1B, TF, HP*, and *CP*) and *RNF10* were validated by quantitative RT-PCR. For the down-regulated genes identified

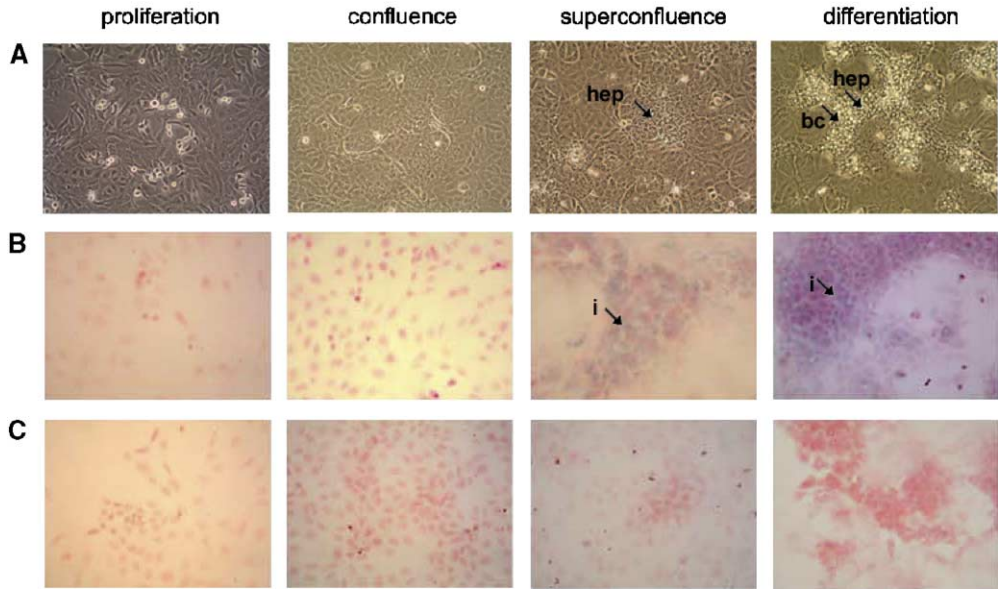

Fig. 1. HepaRG differentiation kinetics and iron storage. Four distinct grades of HepaRG differentiation are followed: proliferation, confluence, superconfluence, and differentiation. (A) Phase-contrast microscopy. Hepatocyte-like cells (hep) become visible during superconfluence and formed colonies with biliary canaliculi (bc). Iron loading capacity is expressed by Perls' staining after addition of 20 μM iron–citrate (B) or 200 μM citrate for the control (C). The presence of iron excess is visible as blue granules within hepatocytes (i). Original magnification, ×100.

by microarray analysis (*SLC11A2, AFP, CYBRD1, TFRC, NFE2L2*, and *DDEF1*), only *NFE2L2* and *DDEF1* were markedly down-regulated in quantitative RT-PCR, whereas *SLC11A2, CYBRD1,* and *TFRC* had weaker modulation profiles than those observed with microarray technology. We could not make any conclusions regarding *SELENBP1* and *AFP*.

Identification of modulated biological processes

Using GoMiner software, we identified 28 Gene Ontology biological processes corresponding to 11 GO classes at level 4 significantly enriched along HepaRG differentiation (Table 3). They corresponded to the following processes: cell growth and/or maintenance, regulation of body fluids, response to stimulus, immune response, cell motility, signal transduction, biosynthesis, energy pathways, and metabolism of macromolecules, lipids, and organic acids. The biological process "cell growth and/or maintenance" was significantly modulated only when cells passed from proliferation to confluence. Then, genes involved in the regulation of body fluids, response to stimulus, and immune response were up-regulated from the proliferation to the superconfluence state. In contrast, when cells reached superconfluence, genes involved in cell motility and signal transduction were repressed. Finally, during final differentiation, the biosynthesis and the energy pathways were down-regulated, whereas genes associated with the metabolism of lipids and organic acids were significantly overexpressed.

Gene expression profiles in HepaRG and hepatocellular carcinoma

To extend results obtained using the HepaRG cell line and cDNA microarray, we analyzed in human samples the expression of some genes implicated in cell motility (*RAC1, MSN, TPM3, FN1*) or in lipid metabolism (*FABP1, CYP4F2, UGT2B7*, and *PLCG2*) in the HepaRG cell line. These genes were respectively repressed and up-regulated along HepaRG differentiation kinetics (Table 3). By testing the gene expression in nontumoral livers versus paired hepatocellular carcinoma, we found that *RAC1, MSN*, and *TPM3* were significantly down-regulated (Fig. 3).

Superconfluence is the critical step for hepatocyte iron accumulation

To reveal the iron storage capacity of the HepaRG line, we exposed the culture to iron–citrate, mimicking the non-transferrin-bound iron found in the plasma of iron-overloaded patients [16,17]. We used Perls' staining to reveal iron excess because this histological method is well correlated with direct chemical measurement [18] and also allowed us to visualize the cell population involved in iron storage (Figs. 1B and 1C). Iron accumulation was visualized neither at proliferation nor at confluent stages, when the culture remained monomorphic. However, at the superconfluence stage, when hepatocyte-like colonies appeared, iron deposits were found within hepatocyte cytoplasm and were present within these cells until final differentiation. In contrast, biliary-like epithelial cells did not exhibit significant iron storage at any stage.

Some biological processes were not associated with iron loading capacity

Under basal culture conditions, we found a strong modulation of biological processes, such as cell growth and/or

Table 2
List of genes which are constantly significantly down-regulated or up-regulated along HepaRG differentiation kinetics

Symbol	Gene Name	GenBank nb	Gene Ontology Biological Processes								
			cell growth and/or maintenance	response to stimulus	immune response	cell motility	signal transduction	energy pathways	biosynthesis	macromolecule metabolism	nucleobase, nucleoside, nucleotide and nucleic acid metabolism
DOWN-REGULATION:											
ATP5B	ATP synthase, H+ transporting, mitochondrial F1 complex, beta	NM_001686	■					■	■		■
DDEF1	development and differentiation enhancing factor 1	NM_018482									■
EEF1A1	eukaryotic translation elongation factor 1 α 1	NM_001402						■		■	
EIF3S6IP	eukaryotic translation initiation factor 3, subunit 6 interacting protein	NM_016091		■				■		■	
EXT1	exostoses (multiple) 1	NM_000127	■				■	■		■	
MSN	moesin	NM_002444	■			■	■			■	
PGD	phosphogluconate dehydrogenase	NM_002631							■	■	■
PTMA	prothymosin, alpha	NM_002823	■								■
RPL10	ribosomal protein L10	NM_006013	■					■		■	
RPLP2	ribosomal protein, large P2	NM_001004						■		■	
SLC25A3	solute carrier family 25, member 3	NM_005888	■						■		
-	cDNA FLJ 31079 fis	AK055641									
-	Sequence 1397 from Patent WO0151513	AX198942									
UP-REGULATION:											
FGL1	fibrinogen-like 1	NM_004467									
HP	haptoglobin	NM_005143	■	■	■	■	■			■	■
TF	transferrin	NM_001063	■	■							■

Level 4 Gene Ontology biological processes corresponding to each gene are represented in grey. Some genes are annotated by several terms, and some others are not annotated.

maintenance, hemostasis, response to stimulus, and immune response (Table 3), when cells passed from proliferation to confluence states. However, these phenotypic modifications were not sufficient to confer iron storage capacity when cells were exposed to iron (Figs. 1B and 1C).

Some biological processes were associated with iron loading capacity

Under basal culture conditions, from confluence to superconfluence, genes involved in hemostasis, response to stimulus, and immune response were still up-regulated, whereas genes involved in cell motility and the protein kinase cascade (signal transduction) were underexpressed (Table 3). At this time, hepatocytes from the HepaRG cell line became able to accumulate iron (Figs. 1B and 1C), suggesting that these processes are involved, or at least are markers of their involvement, in this function.

Finally, under basal culture conditions, from superconfluence to differentiation, during the final differentiation step, genes involved in lipid and fatty acid metabolism were overexpressed and genes involved in biosynthesis, energy pathways, and macromolecule metabolism were down-regulated (Table 3). In addition, in terms of enriched GO molecular functions (data not shown), the overexpression of genes involved in oxidoreductase activity, with a high representation of cytochrome p450 family members (e.g., *CYP3A4, CYP4F2, CYP2E1,* and *CYP2A6*), was significant at this final stage of differentiation (see also Table 4). In parallel, iron loading capacity was maintained during this phase.

Iron metabolism, gene expression, and differentiation status

We focused our analysis on the relationship between iron storage capacity and the expression of genes that were linked to iron metabolism either directly or through their involvement in hematopoiesis or the requirement of iron binding with their protein products for full activity (Table 4). In particular, we identified that the *NFE2L2* gene, involved in hematopoeisis, is

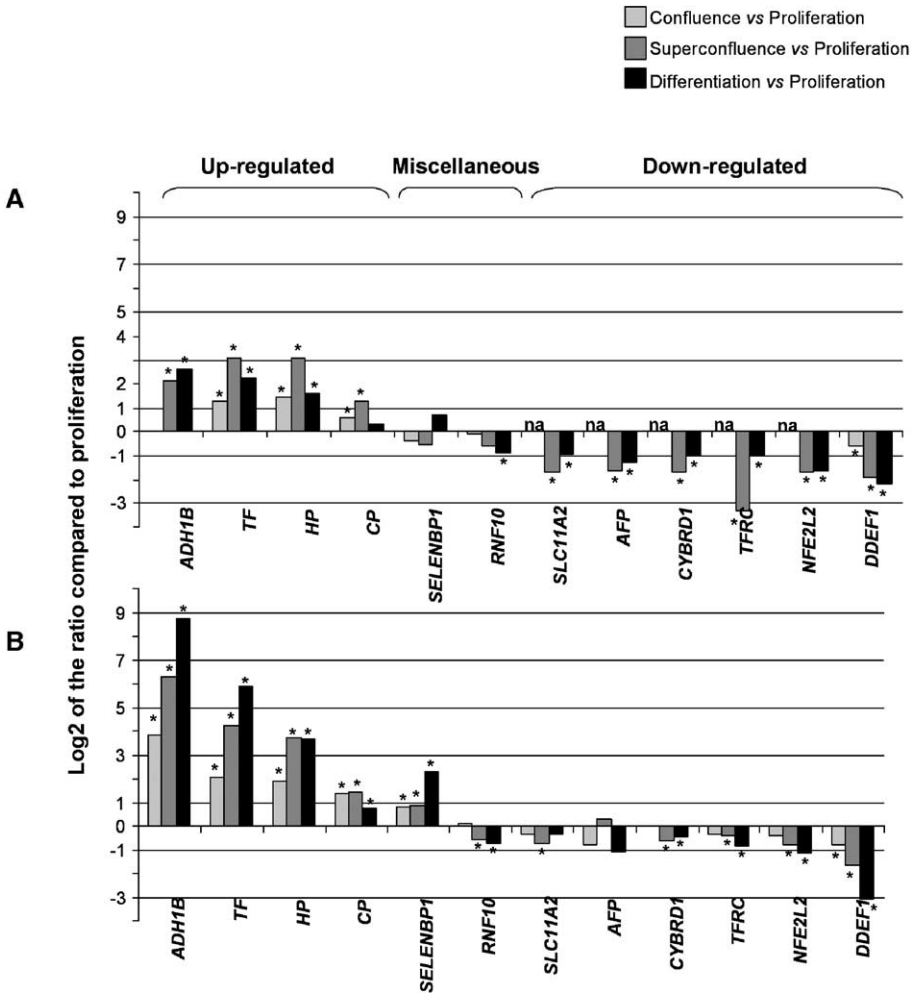

Fig. 2. Validation of hybridization results by quantitative RT-PCR. Values, obtained using microarrays (A) or quantitative RT-PCR (B), of log 2 of the ratio of mRNA levels at the differentiation stage compared to the proliferation stage. na, not available. Significantly modulated genes (*) were selected by Significance Analysis of Microarray and *limma* for microarray results and by the Mann-Whitney test with $P < 0.05$ for quantitative RT-PCR results.

down-regulated during the differentiation process, as well as some genes encoding cytochromes c or other iron-binding proteins (*CYCS, COX7B, COX4I1,* and *MT1G*). In contrast, the expression of genes encoding cytochrome p450 (*CYP3A4, CYP2A6, CYP2E1*, and *CYP4F2*) and plasmatic iron transporters (*HPX, HP*, and *TF*) were up-regulated. Furthermore, the ferritin H gene, involved in iron storage, was down-regulated when HepaRG cells reached superconfluence. Finally, when cells reached differentiation, we noted *CAT* overexpression and *CP* underexpression. For the other genes, no precise pattern was found. The expression patterns of *NFE2L2, HP, TF*, and *CP* were validated by quantitative PCR (Fig. 2).

Discussion

To examine whether there was a relationship between hepatocyte status and iron storage capacity, we analyzed biological processes modulated along HepaRG differentiation in relation to the iron loading capacity of hepatocytes. For this purpose, we used a custom liver microarray and an application combining a statistical tool and gene annotations.

In contrast to other human hepatocyte-derived cell lines, HepaRG cells evolved from an undifferentiated bipotent state to a hepatocyte differentiated state, expressing a very high level of hepatocyte-specific genes and functions similar to those of primary cultures of hepatocytes [13,15]. In this study, we were able to demonstrate that, like human hepatocytes, the HepaRG cell line also supports iron overload. The coherence of the model of HepaRG differentiation with paired hepatocellular carcinoma human samples, based on eight expression pattern profiles (*RAC1, MSN, TPM3, FN1*, *FABP1, CYP4F2, UGT2B7*, and *PLCG2*), illustrated the relevance of this cell line.

Among these eight genes, we identified three genes that were clearly up-regulated in liver tumor versus nontumoral livers. *RAC1* (ras-related C3 botulinum toxin substrate 1), encoding a small GTP-binding protein, is involved in cell motility, cell adhesion, and cytoskeletal reorganization. *MSN* (moesin) is localized in filopodia and membranous protrusions. *TPM3* encodes tropomyosin 3, a protein of the cytoskeleton. All three genes play a role in carcinogenesis [19–21], but none of them have yet been found to be overexpressed in hepatocellular carcinoma. These results lead us to propose

Table 3
Statistical enrichment in some GO biological processes and global modulation of corresponding genes, along HepaRG differentiation

Gene Ontology Terms: biological processes	total array genes number	HepaRG differentiation process		
		Non-iron loading capacity	Iron loading capacity	
		confluence *versus* proliferation	super-confluence *versus* confluence	differentiation *versus* super-confluence
CELL GROWTH/MAINTENANCE	**128**	↑		
positive regulation of cell proliferation	**7**	↑		
regulation of cell proliferation	**11**	↑		
REGULATION OF BODY FLUIDS	**13**			
hemostasis	**12**	↑	↑	
blood coagulation	**12**	↑	↑	
RESPONSE TO STIMULUS	**98**			
response to biotic stimulus	**57**	↑	↑	
defense response	**49**	↑	↑	
response to pest/pathogen/parasite	**36**	↑	↑	
response to external stimulus	**80**	↑	↑	
response to stress	**56**	↑	↑	
response to wounding	**17**		↑	
IMMUNE RESPONSE	**47**	↑	↑	
humoral immune response	**12**		↑	
humoral defense mechanism	**11**		↑	
complement activation	**11**		↑	
acute-phase response	**12**		↑	
innate immune response	**13**		↑	
inflammatory response	**13**		↑	
CELL MOTILITY	**13**		↓	
cell migration	**6**		↓	
SIGNAL TRANSDUCTION	**56**			
protein kinase cascade	**11**		↓	
BIOSYNTHESIS	**67**			↓
macromolecule biosynthesis	**30**			↓
ENERGY PATHWAYS	**41**			↓
MACROMOLECULE METABOLISM	**141**			
translational elongation	**5**			↓
protein biosynthesis	**30**			↓
LIPID METABOLISM	**45**			↑
ORGANIC ACID METABOLISM	**39**			
fatty acid metabolism	**18**			↑

under regulation	↓	$p < 0.01$	$p < 0.001$
over regulation	↑	$p < 0.01$	$p < 0.001$
non significant			

Terms in majuscules and in bold characters are respectively GO terms from levels 4 and 5, others are from lower layers. A color code is given for the statistical p-value of enrichment calculation ($p < 0.01$ in sweet colour, $p < 0.001$ in hard color, blue for non significant enrichment). An arrow code is attributed to gene modulation (overexpression in green, with up-arrow; underexpression in red with down-arrow). A gene can be annotated by several terms.

RAC1, MSN, and *TPM3* as new genes potentially associated with hepatocellular carcinoma.

The HepaRG cell line has a bipotent evolution through hepatocyte-like and biliary-like cells. This dual evolution, which may play a role in the appearance of hepatocyte differentiation due to interactions between both cell types [22], may cause heterogeneity in mRNAs and may lead to a misinterpretation of gene expression profiles. However, contamination by primitive biliary cells does not exceed 40% of the cells at the differentiated state of the culture, based on both immunolocalizations from Parent et al. [14] and phase-contrast microscopy showing large hepatocyte colonies (Fig. 1). Moreover, biliary cell mRNA content is much lower than hepatocyte mRNA content. This is correlated with the weak representativity of biliary-specific genes of our panel of genes selected from suppressive subtractive hybridization libraries from HepaRG differentiation. Thus, our dedicated microarray is an advantage in lessening the impact of the presence of biliary-like cells in the culture. Moreover, under these culture conditions, biliary cells likely correspond to primitive ductular cells [14]. Indeed, of 15 genes previously presented as specific biliary markers [14,23], only 4 are represented in our microarray: *ITGB4* (integrin β4), *ITGA5* (integrin α5), *MME* (or CD10, also named membrane metallo-endopeptidase), and

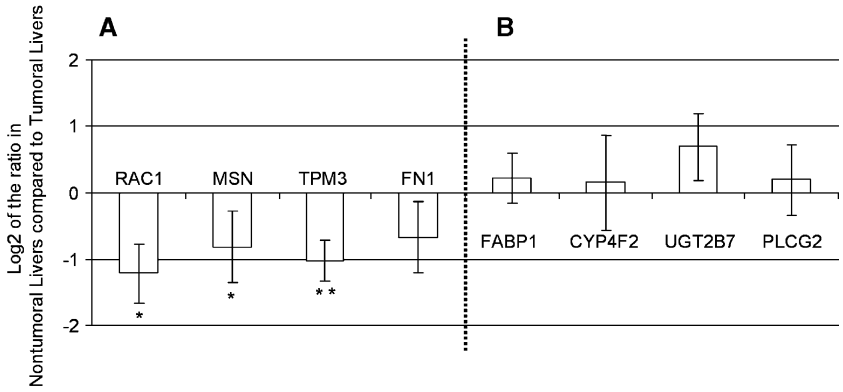

Fig. 3. Gene expression profiles in human hepatocellular carcinoma. Gene expression profiles were studied in 12 cases of human hepatocellular carcinoma. Results are expressed as log 2 of the ratio of mRNA levels in a nontumoral liver area compared to a tumoral area of liver for (A) genes implicated in cell motility and (B) genes implicated in lipid metabolism. mRNA levels of genes implicated in cell motility were down-regulated, whereas those of genes involved in lipid metabolism were globally up-regulated. Significance was attributed for $*P < 0.05$ and $**P < 0.01$ by a paired T test.

CD59 (or protectin). These genes are either down-regulated (*ITGA5* and *CD59*), or invariant (*ITGB4* and *MME*) along HepaRG differentiation kinetics (see gene expression in the Supplementary data found in the online version of this article). Thus, this cDNA microarray reflected more the hepatocyte lineage than the biliary lineage, allowing us to focus our study on the hepatocyte differentiation of the HepaRG cell line in relation to iron storage capacity.

To overcome the truncated view of the whole transcriptome given by our custom microarray, we studied the modulation of biological processes using the GoMiner application to characterize the HepaRG differentiation kinetics. The use

Table 4
Modulation of RNA level of iron metabolism genes along HepaRG differentiation process

Iron relationship	iron modulated	Gene Symbol (Alias)	Iron loading capacity		Gene Name
			Super-confluence *versus* Confluence	Differentiation *versus* Super-Confluence	
hematopoiesis:		*NFE2L2 (NRF2)*	–1.02	–0.64	nuclear factor (erythroid-derived2)-like 2
iron binding:		*CYCS*	–0.89	–1.57	cytochrome c, somatic
		COX7B	na	–0.93	cytochrome c oxidase subunit VIIb
		COX4I1	ns	–1.42	cytochrome c oxidase subunit IV isoform1
		MT1G	ns	–0.45	metallothionein 1G
		SOD1	ns	ns	superoxide dismutase 1, soluble
		TXNL	na	ns	thioredoxin-like, 32kDa
	*	*SCD*	–1.22	0.78	stearoyl-CoA desaturase
		CYP3A4	0.92	3.68	cytochrome P450, family 3, subf. A4
		CYP2A6	ns	1.74	cytochrome P450, family 2, subf. A6
		CYP2E1	na	2.00	cytochrome P450, family 2, subf. E1
		CYP4F2	na	0.71	cytochrome P450, family 4, subf. F2
		CYP4F12	ns	ns	cytochrome P450, family 4, subf. F12
iron metabolism:					
iron binding	*	*TFRC*	na	na	transferrin receptor 1
iron binding	*	*ACO1(IRP1)*	na	na	aconitase-1
iron binding	*	*IREB2 (IRP2)*	ns	na	iron-responsive element binding protein 2
iron binding		*CAT*	na	0.52	catalase
iron oxidoreduction		*CP*	na	–0.91	ceruloplasmin
iron oxidoreduction		*CYBRD1 (DCYTB)*	ns	na	cytochrome b reductase 1
iron storage	*	*FTH1 (FTH)*	–1.97	na	ferritin, heavy polypeptide 1
iron storage	*	*FTL*	na	na	ferritin, light polypeptide
plasmatic iron transport		*HPX*	1.13	0.98	hemopexin
plasmatic iron transport		*HP*	1.80	0.70	haptoglobin
plasmatic iron transport	*	*TF*	1.85	1.07	transferrin

	under regulation
	over regulation
ns	non significant
na	non available data

Differentially expressed genes are selected both by Significance Analysis of Microarray analysis and *limma* analysis. Expression levels are expressed in logarithme base 2 of the ratio indicated in the table.

of a pangenomic microarray would likely lead to the identification of more networks. However, we identified a cluster of genes with a down-regulated expression profile. The association of these genes in a common regulatory network needs further investigation as for the three unannotated genes from the GO biological process (GenBank Accession Nos. AK055641, AX198942, and NM_004467). The roles of these genes in HepaRG differentiation kinetics remain to be defined.

We demonstrate that modulation of cell motility, response to stimulus, and immune response gene expression (at the confluence and superconfluence stages) clearly preceded the expression of massive hepatocyte functions (at the differentiation stage). Modulated genes at these stages of differentiation are potential candidates for the appearance of the hepatocyte phenotype, as occurring in coculture by interactions between hepatocytes and biliary cells [22].

Both HepaRG differentiation and liver regeneration require the orchestration of pathways controlling cell differentiation and proliferation. We found, comparing two different studies [24,25] that examined mice regenerating livers, a similar expression profile for genes implicated in the acute-phase response and inflammatory response, among them *ORM1* (α-1 acid glycoprotein 1B), *ORM2, FGA*, and *FGB,* which are overexpressed in mice regenerating livers and in HepaRG cells, at least until superconfluence. In the same way, the expression of hepatic lipid accumulation is specifically regulated during liver regeneration [26], which parallels the overexpression of lipid metabolism genes along HepaRG differentiation. This suggests that the HepaRG cell line could be a valuable model for studying the hepatocyte regeneration process. An alteration of normal expression of these genes could play a role in the development of liver diseases, especially during hepatic regeneration and oxidative stress.

In this work, we found that HepaRG cells cannot undergo iron loading when genes involved in cell proliferation are highly expressed. In contrast, HepaRG iron load capacity occurs with the appearance of hepatocyte-like cells and is maintained at the highest differentiated stage. This iron storage capacity can be first associated with the down-regulation of genes implicated in cell motility and in the protein kinase cascade. This sharp dichotomy—non-iron load capacity linked to high cell growth and/or maintenance activity as opposed to iron load capacity related to a decrease in motility and migration capacity—is in accordance with clinical observations in hepatocellular carcinoma. Indeed, proliferative, i.e., potentially more motile, hepatocellular carcinoma cells are always iron-poor, even if the corresponding nontumoral liver is iron-overloaded [12]. This is also consistent with the description of the iron-poor phenotype of iron-free foci, which are proliferative and potential preneoplastic lesions, in the nontumoral liver of untreated genetic hemochromatosis patients [27,28]. Iron overload capacity is also associated with the up-regulation of genes involved in the response to stress and the immune response, suggesting that some of these genes are required to protect hepatocytes against pathogens and exogenous agents, including iron excess. Finally, the absence of stainable iron in biliary-like cells fits well with the delay of the iron overload of biliary cells compared to hepatocytes in human liver iron overload especially during genetic hemochromatosis [28].

Our data demonstrate that the iron storage behavior of HepaRG cells depends on the hepatocyte differentiation status. These data are consistent with a previous report showing that differentiation in CaCo-2 cells, a model of enterocytes and implicated in iron absorption, is associated with a decrease in the expression of genes involved in the cell cycle and with signal transduction, whereas an increase in the expression of genes linked to lipid metabolism and the immune response, as well as the modulation of genes involved in iron metabolism, was reported [29].

Concerning gene modulation in iron metabolism, during the evolution from HepaRG confluence to superconfluence in the absence of iron supplementation, an increased expression was found for hemopexin, haptoglobin, and transferrin genes, which encode iron plasmatic transporters, suggesting their association with iron storage capacity. Conversely, the expression of ferritin H (*FTH1*) and *NFE2L2* (also named *NRF2*) mRNAs decreased. The NFE2L2 transcription factor is known to regulate the expression of some iron metabolism genes, such as *HMOX1*, *TXNL*, *SOD1*, and *CAT* [30], and could also mediate the transcriptional induction of *FTH1* and *FTL* mRNAs [31]. Although *FTH1* mRNA is also known to be translationally regulated through iron regulatory proteins, encoded by *ACO1* and *IREB2* genes [7], the similarity in expression patterns between the *NFE2L2* and *FTH1* genes in HepaRG cells evokes, in humans, the possible transcriptional control of the *FTH1* gene by the NFE2L2 transcription factor, suggesting the involvement of *NFE2L2* in iron storage capacity in the liver. This hypothesis is reinforced by a recent report demonstrating that *Nrf2*−/− mice had an increase in liver iron content [32].

In conclusion, our study demonstrates that hepatocyte iron loading capacity is strongly associated with both the decrease in cell motility and the appearance of highly differentiated hepatocyte functions including xenobiotic metabolism, lipid metabolism, or response to stress. We also highlight new genes associated with the hepatocyte differentiation process and propose new genes potentially related to hepatocellular carcinoma. Taken together, these data suggest that identified biological processes and related genes represent good candidates for the understanding of: (i) the relationship between iron metabolism and hepatocyte differentiated status and (ii) the switch between hepatocyte differentiation and proliferation, especially during liver regeneration. They could lead to the identification of new diagnostic or therapeutic targets useful for the follow-up of patients with chronic liver diseases.

Materials and methods

HepaRG cell culture, iron exposure, and Perls' staining

The HepaRG cell line was cultured in basal medium as previously described [13]. We considered four distinct stages of the differentiation process: proliferating cells (day 3 postspreading), confluent cells (days 5 and 6),

superconfluent cells (days 12–15), and finally differentiated cells (day 30 with the last 15 days in basal medium supplemented with 2% dimethylsulfoxide). When applicable, exposure to iron excess was performed using 20 μM iron–citrate (1 iron/10 citrate) [33] or 200 μM citrate as control for 48 h with a daily renewed culture medium at the four distinct stages of differentiation. Perls' staining revealed an excess of intracellular iron [34].

Construction of the human liver dedicated cDNA microarray

We performed four suppressive subtractive hybridization libraries [35] with the PCR Select cDNA Subtraction Kit (Clontech, Palo Alto, CA) on human hepatocarcinoma samples versus nontumoral human livers, obtained in accordance with French laws and regulations, and on HepaRG cells at proliferation versus differentiation stages. Clones were sequenced at Genoscope (Evry, France) and massive BLASTs were performed with PCIO informatics facilities (Rennes, France). A total of 2436 PCR-amplified cDNA clones, supplemented with 36 PCR-amplified iron metabolism cDNAs and several controls [human β-actin cDNA, cDNAs corresponding to *Cab, RCA*, or *rbcl* genes from *Arabidopsis thaliana* (Spot Report Array Validation System, Stratagene)], corresponding to 584 human distinct genes (the list of genes is available at http://u522.rennes.inserm.fr/donnees/troadec.htm), were spotted in duplicate onto precoated glass slides (CMT-GAPS, Corning).

Poly(A) RNA isolation and fluorescence labeling

Total RNAs were isolated by ultracentrifugation under denaturing conditions [36]. RNA quality was assayed by electrophoresis migration on agarose gel. The absence of genomic DNA was verified by PCR using human β-actin primers and by using a lab chip device (Agilent 2100 Bioanalyzer). Poly(A) RNAs were extracted with a large-scale mRNA isolation kit (Miltenyi Biotec). The quality and quantity of purified poly(A) were assayed on the Agilent 2100 Bioanalyzer. Poly(A)s were then labeled using a CyScribe Postlabeling Kit (Amersham) according to the manufacturer's instructions. Each sample was labeled with Cy3 dye and then with Cy5 dye, for further dye-swap hybridizations.

Experimental design, hybridization, and scanning

We compared the four stages of differentiation in a loop design (Fig. 4) and performed two independent experiments. Each hybridization was performed in dye-swap. We followed the hybridization protocol available on the Web (http://cardioserve.nantes.inserm.fr/ptf-puce/) (protocols 7 and 9). Fluorescence was read on a ScanArray Express 4000 XL (Packard Bioscience). Image analyses were performed with Genepix Pro 4.0 (Axon, Union City, USA).

Data processing

Raw data, expressed as log 2 of the expression ratio, were preprocessed through the MADSCAN application available on the Web [29,37] by the *lowess* fitness normalization and a scaling on the internal variance of each replicated array. To remove nonreproducible values, data were then processed on replicated spots in a single array, on replicated arrays, and finally on redundant genes. Heterogeneous spots, signals below the detection level, and insufficiently reproducible values were identified as not available (na).

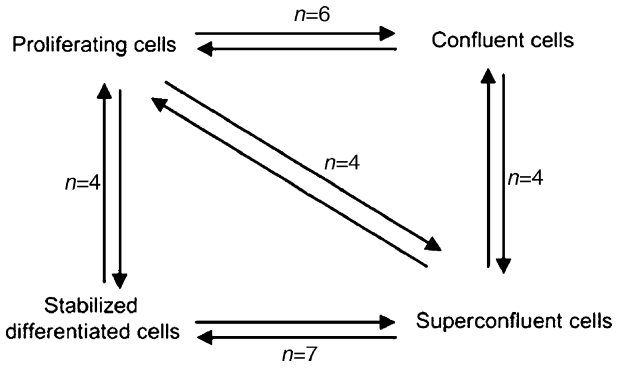

Fig. 4. Experimental design of hybridizations performed in this study. *n* denotes the number of different hybridizations; double arrows represent dye-swap hybridizations.

Identification of differentially expressed genes

We combined two methods to point out differentially expressed genes. In the Significance Analysis of Microarray method (SAM) [38], the cut-off for significance was determined by the minimal false discovery rate calculated between our data and a randomized matrix of these data. In the *limma* method, available in the R-package [39], which lies on an empirical Bayes moderated *T* test, the cut-off for significance is a *P* value of less than 0.05. Significantly differentially expressed genes were the common list of differentially expressed genes selected by both SAM analysis and *limma* analysis.

Statistical enrichment of biological processes

The Gene Ontology Consortium [40] annotates the genome through categories of biological processes. Annotations are organized in a tree-like structure with several levels. The calculation of statistical enrichment of GO annotations of significantly modulated genes compared to total array genes at every level of the GO hierarchy was delivered through the GoMiner application available on the Web [41]. The statistical calculation consisted of a two-sided *P* value from Fisher's exact test between the total set of the gene array and the subset of significantly modulated genes. A *P* value of less than 0.01 was considered statistically significant.

Quantitative real-time RT-PCR validation

Twenty genes were selected for validation using quantitative real-time PCR. Primer design was performed with the assistance of Primer Express software (PE Biosystems). These genes were as follows: *ADH1B, AFP, CP, CYBRD1, CYP4F2, DDEF1, FABP1, FN1, HP, MSN, NFE2L2, PLCG2, RAC1, RNF10, SELENBP1, SLC11A2, TF, TFRC, TPM3*, and *UGT2B7.* Primers are available at http://u522.rennes.inserm.fr/donnees/troadec.html. All quantitative real-time PCR assays were performed using qPCR core reagent kit for SybrGreen1 (Eurogentec, Belgium) on an ABI Prism 7000 SDS (Applied Bioscience, London, UK): 95°C for 10 min followed by 40 cycles of 95°C for 15 s and 60°C for 1 min. Expression data were normalized using 18S rRNA endogenous reference.

Human liver samples

Paired nontumoral and tumoral liver samples of 12 patients operated on for hepatocellular carcinoma were obtained from the Biological Resource Center of Rennes after local ethical committee approval and after obtaining informed consent from patients. Total RNA extraction and reverse transcription were performed as previously described [42].

Statistical analysis

For quantitative PCR results, the Mann-Whitney test or paired *T* test were performed by StatView software. Significance was attributed for $P < 0.05$.

Acknowledgments

We thank OUEST Genopole and IFR 140 for transcriptome core facilities, the Biological Resource Center for supplying human samples, and Dr. B. Turlin (pathologist). This work was supported by a PRIR (No. 139) of the Région Bretagne, the French Ministry of Research and Technology (M.B.T. and

E.G.), the Association Fer et Foie, and the European Community QLRT-2001-00444 contract.

Appendix A. Supplementary data

Supplementary data associated with this article can be found in the online version at doi:10.1016/j.ygeno.2005.08.016.

References

[1] P. Aisen, A. Leibman, R.A. Pinkowitz, The anion-binding functions of transferrin, Adv. Exp. Med. Biol. 48 (1974) 125–140.
[2] A. vander Straten, A. Herzog, P. Jacobs, T. Cabezon, A. Bollen, Molecular cloning of human haptoglobin cDNA: Evidence for a single mRNA coding for alpha 2 and beta chains, EMBO J. 2 (1983) 1003–1007.
[3] S.L. Naylor, F. Altruda, A. Marshall, L. Silengo, B.H. Bowman, Hemopexin is localized to human chromosome 11, Somat. Cell. Mol. Genet. 13 (1987) 355–358.
[4] C. Pigeon, G. Ilyin, B. Courselaud, P. Leroyer, B. Turlin, P. Brissot, O. Loréal, A new mouse liver-specific gene, encoding a protein homologous to human antimicrobial peptide hepcidin, is overexpressed during iron overload, J. Biol. Chem. 276 (2001) 7811–7819.
[5] C.M. Craven, J. Alexander, M. Eldridge, J.P. Kushner, S. Bernstein, J. Kaplan, Tissue distribution and clearance kinetics of non-transferrin-bound iron in the hypotransferrinemic mouse: A rodent model for hemochromatosis, Proc. Natl. Acad. Sci. USA 84 (1987) 3457–3461.
[6] P. Brissot, T.L. Wright, W.L. Ma, R.A. Weisiger, Efficient clearance of non-transferrin-bound iron by rat liver. Implications for hepatic iron loading in iron overload states, J. Clin. Invest. 76 (1985) 1463–1470.
[7] E.C. Theil, Ferritin: Structure, gene regulation, and cellular function in animals, plants, and microorganisms, Annu. Rev. Biochem. 56 (1987) 289–315.
[8] J.N. Feder, A. Gnirke, W. Thomas, Z. Tsuchihashi, D.A. Ruddy, A. Basava, F. Dormishian, R. Domingo Jr., M.C. Ellis, A. Fullan, L.M. Hinton, N.L. Jones, B.E. Kimmel, G.S. Kronmal, P. Lauer, V.K. Lee, D.B. Loeb, F.A. Mapa, E. McClelland, N.C. Meyer, G.A. Mintier, N. Moeller, T. Moore, E. Morikang, R.R. Wolff, et al., A novel MHC class I-like gene is mutated in patients with hereditary haemochromatosis, Nat. Genet. 13 (1996) 399–408.
[9] P. Brissot, Y. Deugnier, Haemochromatosis, in: J. Bircher, J.P. Benhamou, N. Mcintyre, M. Rizetto, J. Rodes (Eds.), Oxford Textbook of Clinical Hepatology, Oxford University Press, 1999, pp. 1379–1391.
[10] C. Niederau, R. Fischer, A. Sonnenberg, W. Stremmel, H.J. Trampisch, G. Strohmeyer, Survival and causes of death in cirrhotic and in noncirrhotic patients with primary hemochromatosis, N. Engl. J. Med. 313 (1985) 1256–1262.
[11] Y. Deugnier, B. Turlin, D. le Quilleuc, R. Moirand, O. Loreal, M. Messner, B. Meunier, P. Brissot, B. Launois, A reappraisal of hepatic siderosis in patients with end-stage cirrhosis: Practical implications for the diagnosis of hemochromatosis, Am. J. Surg. Pathol. 21 (1997) 669–675.
[12] B. Turlin, F. Juguet, R. Moirand, D. Le Quilleuc, O. Loreal, J.P. Campion, B. Launois, M.P. Ramee, P. Brissot, Y. Deugnier, Increased liver iron stores in patients with hepatocellular carcinoma developed on a noncirrhotic liver, Hepatology 22 (1995) 446–450.
[13] P. Gripon, S. Rumin, S. Urban, J. Le Seyec, D. Glaise, I. Cannie, C. Guyomard, J. Lucas, C. Trepo, C. Guguen-Guillouzo, Infection of a human hepatoma cell line by hepatitis B virus, Proc. Natl. Acad. Sci. USA 99 (2002) 15655–15660.
[14] R. Parent, M.J. Marion, L. Furio, C. Trepo, M.A. Petit, Origin and characterization of a human bipotent liver progenitor cell line, Gastroenterology 126 (2004) 1147–1156.
[15] P. Gripon, I. Cannie, S. Urban, Efficient inhibition of hepatitis B virus infection by acylated peptides derived from the large viral surface protein, J. Virol. 79 (2005) 1613–1622.
[16] M. Grootveld, J.D. Bell, B. Halliwell, O.I. Aruoma, A. Bomford, P.J. Sadler, Non-transferrin-bound iron in plasma or serum from patients with idiopathic hemochromatosis. Characterization by high performance liquid chromatography and nuclear magnetic resonance spectroscopy, J. Biol. Chem. 264 (1989) 4417–4422.
[17] R.C. Hider, Nature of nontransferrin-bound iron, Eur. J. Clin. Invest. 32 (Suppl. 1) (2002) 50–54.
[18] Y.M. Deugnier, B. Turlin, L.W. Powell, K.M. Summers, R. Moirand, L. Fletcher, O. Loréal, P. Brissot, J.W. Halliday, Differentiation between heterozygotes and homozygotes in genetic hemochromatosis by means of a histological hepatic iron index: A study of 192 cases, Hepatology 17 (1993) 30–34.
[19] S. Aznar, J.C. Lacal, Rho signals to cell growth and apoptosis, Cancer Lett. 165 (2001) 1–10.
[20] H. Kobayashi, J. Sagara, H. Kurita, M. Morifuji, M. Ohishi, K. Kurashina, S. Taniguchi, Clinical significance of cellular distribution of moesin in patients with oral squamous cell carcinoma, Clin. Cancer Res. 10 (2004) 572–580.
[21] L. Lamant, N. Dastugue, K. Pulford, G. Delsol, B. Mariame, A new fusion gene TPM3-ALK in anaplastic large cell lymphoma created by a (1;2) (q25;p23) translocation, Blood 93 (1999) 3088–3095.
[22] J.M. Fraslin, B. Kneip, S. Vaulont, D. Glaise, A. Munnich, C. Guguen-Guillouzo, Dependence of hepatocyte-specific gene expression on cell–cell interactions in primary culture, EMBO J. 4 (1985) 2487–2491.
[23] J.Y. Scoazec, A.F. Bringuier, J.F. Medina, E. Martinez-Anso, D. Veissiere, G. Feldmann, C. Housset, The plasma membrane polarity of human biliary epithelial cells: in situ immunohistochemical analysis and functional implications, J. Hepatol. 26 (1997) 543–553.
[24] N. Kelley-Loughnane, G.E. Sabla, C. Ley-Ebert, B.J. Aronow, J.A. Bezerra, Independent and overlapping transcriptional activation during liver development and regeneration in mice, Hepatology 35 (2002) 525–534.
[25] M. Arai, O. Yokosuka, T. Chiba, F. Imazeki, M. Kato, J. Hashida, Y. Ueda, S. Sugano, K. Hashimoto, H. Saisho, M. Takiguchi, N. Seki, Gene expression profiling reveals the mechanism and pathophysiology of mouse liver regeneration, J. Biol. Chem. 278 (2003) 29813–29818.
[26] E. Shteyer, Y. Liao, L.J. Muglia, P.W. Hruz, D.A. Rudnick, Disruption of hepatic adipogenesis is associated with impaired liver regeneration in mice, Hepatology 40 (2004) 1322–1332.
[27] Y.M. Deugnier, P. Charalambous, D. Le Quilleuc, B. Turlin, J. Searle, P. Brissot, L.W. Powell, J.W. Halliday, Preneoplastic significance of hepatic iron-free foci in genetic hemochromatosis: a study of 185 patients, Hepatology 18 (1993) 1363–1369.
[28] Y.M. Deugnier, O. Loréal, B. Turlin, D. Guyader, H. Jouanolle, R. Moirand, C. Jacquelinet, P. Brissot, Liver pathology in genetic hemochromatosis: A review of 135 homozygous cases and their bioclinical correlations, Gastroenterology 102 (1992) 2050–2059.
[29] H. Bedrine-Ferran, N. Le Meur, I. Gicquel, M. Le Cunff, N. Soriano, I. Guisle, S. Mottier, A. Monnier, R. Teusan, P. Fergelot, J.Y. Le Gall, J. Leger, J. Mosser, Transcriptome variations in human CaCo-2 cells: A model for enterocyte differentiation and its link to iron absorption, Genomics 83 (2004) 772–789.
[30] K. Chan, X.D. Han, Y.W. Kan, An important function of Nrf2 in combating oxidative stress: Detoxification of acetaminophen, Proc. Natl. Acad. Sci. USA 98 (2001) 4611–4616.
[31] E.C. Pietsch, J.Y. Chan, F.M. Torti, S.V. Torti, Nrf2 mediates the induction of ferritin H in response to xenobiotics and cancer chemopreventive dithiolethiones, J. Biol. Chem. 278 (2003) 2361–2369.
[32] T. Yanagawa, K. Itoh, J. Uwayama, Y. Shibata, A. Yamaguchi, T. Sano, T. Ishii, H. Yoshida, M. Yamamoto, Nrf2 deficiency causes tooth decolourization due to iron transport disorder in enamel organ, Genes Cells 9 (2004) 641–651.
[33] P. Azari, R.F. Baugh, A simple and rapid procedure for preparation of large quantities of pure ovotransferrin, Arch. Biochem. Biophys. 118 (1967) 128–144.
[34] R. Hould, Techniques d'histopathologie et de cytopathologie, Décarie, Montréal.
[35] L. Diatchenko, Y.F. Lau, A.P. Campbell, A. Chenchik, F. Moqadam, B. Huang, S. Lukyanov, K. Lukyanov, N. Gurskaya, E.D. Sverdlov, P.D.

Siebert, Suppression subtractive hybridization: A method for generating differentially regulated or tissue-specific cDNA probes and libraries, Proc. Natl. Acad. Sci. USA 93 (1996) 6025–6030.

[36] J.M. Chirgwin, A.E. Przybyla, R.J. MacDonald, W.J. Rutter, Isolation of biologically active ribonucleic acid from sources enriched in ribonuclease, Biochemistry 18 (1979) 5294–5299.

[37] N. Le Meur, G. Lamirault, A. Bihouee, M. Steenman, H. Bedrine-Ferran, R. Teusan, G. Ramstein, J.J. Leger, A dynamic, web-accessible resource to process raw microarray scan data into consolidated gene expression values: Importance of replication, Nucleic Acids Res. 32 (2004) 5349–5358.

[38] V.G. Tusher, R. Tibshirani, G. Chu, Significance analysis of microarrays applied to the ionizing radiation response, Proc. Natl. Acad. Sci. USA 98 (2001) 5116–5121.

[39] R. Ihaka, R. Gentleman, R: A language for data analysis and graphics, J. Comput. Graph. Stat. 5 (1996) 299–314.

[40] M. Ashburner, C.A. Ball, J.A. Blake, D. Botstein, H. Butler, J.M. Cherry, A.P. Davis, K. Dolinski, S.S. Dwight, J.T. Eppig, M.A. Harris, D.P. Hill, L. Issel-Tarver, A. Kasarskis, S. Lewis, J.C. Matese, J.E. Richardson, M. Ringwald, G.M. Rubin, G. Sherlock, Gene ontology: Tool for the unification of biology. The Gene Ontology Consortium, Nat. Genet. 25 (2000) 25–29.

[41] B.R. Zeeberg, W. Feng, G. Wang, M.D. Wang, A.T. Fojo, M. Sunshine, S. Narasimhan, D.W. Kane, W.C. Reinhold, S. Lababidi, K.J. Bussey, J. Riss, J.C. Barrett, J.N. Weinstein, GoMiner: A resource for biological interpretation of genomic and proteomic data, Genome Biol. 4 (2003) R28.

[42] L. Detivaud, E. Nemeth, K. Boudjema, B. Turlin, M.B. Troadec, P. Leroyer, M. Ropert, S. Jacquelinet, B. Courselaud, T. Ganz, P. Brissot, O. Loréal, Hepcidin levels in humans are correlated with hepatic iron stores, hemoglobin levels and hepatic function, Blood 106 (2005) 746–748.